Design of fixed-structure controllers with frequency-domain criteria: a multiobjective optimisation approach

H.T. Toivonen and S. Tötterman

Abstract: An optimisation-based iterative design of fixed-structure controllers with frequency-domain criteria is presented. An interactive multiobjective optimisation procedure is presented, which is based on a direct shaping of the frequency responses, without the need to construct explicit weighting filters. At each iteration, a constrained optimisation problem is formulated in such a way that successive improvements of the design to meet the designer's specifications are achieved. For computational efficiency, time-domain expressions consisting of linear matrix equations are used to characterise the frequency responses.

1 Introduction

Frequency response shaping has been found useful in the design of controllers with good performance and robustness properties, see for example [1, 2]. The frequency response specifications are typically characterised in terms of a number of closed-loop transfer functions $T_i(s)$, $i = 1, \ldots, N$, such as the sensitivity and the complementary sensitivity functions, as well as various input-output transfer functions. For a satisfactory performance and robustness, it is required that the responses satisfy certain frequency-dependent bounds,

$$\|T_i(j\omega)\| \leq l_i(\omega), \quad i = 1, \ldots, N \tag{1}$$

The appropriate bounds are, however, seldom known *a priori*, because the trade-offs between the various frequency responses are unknown. Therefore, the controller design problem is an inherently iterative process.

In H_∞ loop-shaping techniques, controllers which achieve the frequency-response bounds are computed by solving H_∞-optimal control problems with appropriate weighting filters to shape the closed-loop transfer functions [3, 4]. The design can be made in a systematic way by selecting the weighting filters in such a way that satisfactory frequency responses are achieved. This procedure has, however, some shortcomings. Firstly, it is not known *a priori* how much a change in the weighting filters will affect the closed-loop responses, leading easily to an elaborate iterative process. Secondly, the optimal controller has the same order as the generalised plant, including the weighting filters. Therefore, controllers with excessively high orders are often obtained. In practice one is often interested in the optimal tuning of a controller of fixed order or structure, such as a proportional-integral-derivative (PID) controller, and the loop-shaping technique does not directly address this kind of problem. Although there are methods for controller reduction [3, 4], the controller order cannot be reduced too much without a degradation of control performance. Therefore, these methods are in general not suitable for example to the problem of finding an optimally tuned PID controller.

An alternative is to solve the reduced-order optimal control problem directly. The reduced-order H_∞-optimal control problem is, however, numerically very demanding [5, 6]. Therefore, it is not well suited for a design process where the weighting filters are tuned iteratively. One way to overcome these limitations is to optimise the closed-loop frequency responses directly assuming a fixed-structure controller, without introducing any explicit weighting filters, cf. [7, 8].

In addition to the problems discussed above, it should be observed that the controller design problem is clearly a multiple objective optimisation problem, in which a number of conflicting objectives should be taken into account. The most satisfactory achievable design is in general not known in advance. Therefore, the controller design is typically an iterative process aimed at finding a satisfactory trade-off between the various design objectives. Multiobjective optimisation methods provide systematic tools for iterative controller design involving several objectives, see for example [9–13] and the references therein.

In this study, we consider a multiobjective controller design approach for fixed-structure controllers, which is based on direct shaping of the closed-loop frequency responses, without the need to construct weighting filters. The proposed interactive design method is based on the solution of a sequence of constrained optimisation problems, which are defined in such a way that a more satisfactory design is obtained at each stage.

An important feature of the proposed method is that the frequency-domain costs are characterised in terms of state-space expressions defined in the time domain. In this way all the calculations can be based on real-valued arithmetics. The time-domain expressions consist of linear matrix equations, which are similar to the matrix Lyapunov equations used to evaluate quadratic costs in linear quadratic control. In this study, the time-domain expressions are used to derive gradients of the frequency-domain costs with respect to the controller parameters. The optimisation problems involved in the design process can then be solved

IEE Proceedings online no. 20045103

doi:10.1049/ip-cta:20045103

Paper first received 30th June 2004 and in revised form 14th March 2005

The authors are with Department of Chemical Engineering, Åbo Akademi University, FIN-20500 Åbo, Finland

E-mail: Hannu.Toivonen@abo.fi

using powerful numerical optimisation techniques, similar to those applied in optimal parametric linear quadratic control problems [14].

2 Time-domain expressions for the frequency responses

In this Section, time-domain expressions for the closed-loop frequency responses and their gradients with respect to the controller parameters are derived. We consider the time-delay system:

$$\begin{aligned}\dot{\boldsymbol{x}}_P(t) &= \boldsymbol{A}_P\boldsymbol{x}_P(t) + \boldsymbol{B}_{P,1}v(t) + \boldsymbol{B}_{P,2}u(t-\tau)\\ z(t) &= \boldsymbol{C}_{P,1}\boldsymbol{x}_P(t) + \boldsymbol{D}_{P,11}v(t) + \boldsymbol{D}_{P,12}u(t-\tau)\\ y(t) &= \boldsymbol{C}_{P,2}\boldsymbol{x}_P(t) + \boldsymbol{D}_{P,21}v(t)\end{aligned} \tag{2}$$

where $\boldsymbol{x}_P$ is the state vector, v is a disturbance, u is the control signal, and z and y are the controlled and measured output signals. It is assumed that the controller has the state-space representation:

$$\begin{aligned}\dot{\boldsymbol{x}}_c(t) &= A_c\boldsymbol{x}_c(t) + B_c y(t)\\ u(t) &= C_c\boldsymbol{x}_c(t) + D_c y(t)\end{aligned} \tag{3}$$

Introducing the augmented state $\boldsymbol{x} = [\boldsymbol{x}_P^T,\ \boldsymbol{x}_c^T]^T$ and the matrices:

$$\begin{aligned}&\boldsymbol{A} = \begin{bmatrix}\boldsymbol{A}_P & 0\\ 0 & 0\end{bmatrix}\\ &\boldsymbol{B}_1 = \begin{bmatrix}\boldsymbol{B}_{P,1}\\ 0\end{bmatrix},\quad \boldsymbol{B}_{21} = \begin{bmatrix}0 & 0\\ \boldsymbol{I} & 0\end{bmatrix},\quad \boldsymbol{B}_{22} = \begin{bmatrix}0 & \boldsymbol{B}_{P,2}\\ 0 & 0\end{bmatrix}\\ &\boldsymbol{C}_1 = \begin{bmatrix}\boldsymbol{C}_{P,1} & 0\end{bmatrix},\quad \boldsymbol{C}_2 = \begin{bmatrix}0 & \boldsymbol{I}\\ \boldsymbol{C}_{P,2} & 0\end{bmatrix}\\ &\boldsymbol{D}_{11} = \boldsymbol{D}_{P,11},\quad \boldsymbol{D}_{12} = \begin{bmatrix}0 & \boldsymbol{D}_{P,12}\end{bmatrix},\quad \boldsymbol{D}_{21} = \begin{bmatrix}0\\ \boldsymbol{D}_{P,21}\end{bmatrix}\end{aligned} \tag{4}$$

the closed-loop system (2), (3) is described by

$$\begin{aligned}\dot{\boldsymbol{x}}(t) &= \boldsymbol{A}_0(\boldsymbol{F})\boldsymbol{x}(t) + \boldsymbol{A}_\tau(\boldsymbol{F})\boldsymbol{x}(t-\tau) + \boldsymbol{B}_0(\boldsymbol{F})v(t)\\ &\quad + \boldsymbol{B}_\tau(\boldsymbol{F})v(t-\tau)\\ z(t) &= \boldsymbol{C}(F)\boldsymbol{x}(t) + \boldsymbol{D}(\boldsymbol{F})v(t)\end{aligned} \tag{5}$$

where $\boldsymbol{F}$ is a matrix consisting of the controller parameters,

$$\boldsymbol{F} = \begin{bmatrix}A_c & \boldsymbol{B}_c\\ \boldsymbol{C}_c & \boldsymbol{D}_c\end{bmatrix} \tag{6}$$

and

$$\begin{aligned}\boldsymbol{A}_0(\boldsymbol{F}) &= \boldsymbol{A} + \boldsymbol{B}_{21}\boldsymbol{F}\boldsymbol{C}_2,\quad \boldsymbol{A}_\tau(\boldsymbol{F}) = \boldsymbol{B}_{22}\boldsymbol{F}\boldsymbol{C}_2\\ \boldsymbol{B}_0(\boldsymbol{F}) &= \boldsymbol{B}_1 + \boldsymbol{B}_{21}\boldsymbol{F}\boldsymbol{D}_{21},\quad \boldsymbol{B}_\tau(\boldsymbol{F}) = \boldsymbol{B}_{22}\boldsymbol{F}\boldsymbol{D}_{21}\\ \boldsymbol{C}(\boldsymbol{F}) &= \boldsymbol{C}_1 + \boldsymbol{D}_{12}\boldsymbol{F}\boldsymbol{C}_2,\quad \boldsymbol{D}(\boldsymbol{F}) = \boldsymbol{D}_{11} + \boldsymbol{D}_{12}\boldsymbol{F}\boldsymbol{D}_{21}\end{aligned} \tag{7}$$

In order to obtain a time-domain, state-space expression for the frequency response of (5), observe that a scalar-valued sinusoidal input signal $v(t) = \sin(\omega t)$ can be described by the state-space model:

$$\begin{aligned}\dot{\boldsymbol{x}}_v(t) &= \boldsymbol{A}_v(\omega)\boldsymbol{x}_v(t)\\ v(t) &= \boldsymbol{C}_v\boldsymbol{x}_v(t)\end{aligned} \tag{8}$$

where $\boldsymbol{x}_v(t) = [\sin(\omega t)\quad \cos(\omega t)]^T$ and

$$\boldsymbol{A}_v(\omega) = \begin{bmatrix}0 & \omega\\ -\omega & 0\end{bmatrix},\quad \boldsymbol{C}_v = \begin{bmatrix}1 & 0\end{bmatrix} \tag{9}$$

We then have the following result.

Theorem 1: The steady-state response of the system (5) to the disturbance (8) is given by:

$$\boldsymbol{x}(t) = \boldsymbol{E}_\omega(\boldsymbol{F})\boldsymbol{x}_v(t) \tag{10}$$

where the $\dim(\boldsymbol{x}) \times 2$ matrix $\boldsymbol{E}_\omega(\boldsymbol{F})$ is the solution of the linear matrix equation:

$$\begin{aligned}&\boldsymbol{A}_0(\boldsymbol{F})\boldsymbol{E}_\omega(\boldsymbol{F}) + \boldsymbol{A}_\tau(\boldsymbol{F})\boldsymbol{E}_\omega(\boldsymbol{F})e^{-\boldsymbol{A}_v(\omega)\tau} - \boldsymbol{E}_\omega(\boldsymbol{F})\boldsymbol{A}_v(\omega)\\ &\quad + \boldsymbol{B}_0(\boldsymbol{F})\boldsymbol{C}_v + \boldsymbol{B}_\tau(\boldsymbol{F})\boldsymbol{C}_v e^{-\boldsymbol{A}_v(\omega)\tau} = 0\end{aligned} \tag{11}$$

Proof: In the steady state, the states $\boldsymbol{x}(t)$ are linear combinations of the components of $\boldsymbol{x}_v(t)$, i.e. there exists a matrix $\boldsymbol{E}_\omega(\boldsymbol{F})$ such that (10) holds. Using (5), (10) and (8), we have the identity:

$$\begin{aligned}\dot{\boldsymbol{x}}(t) &= \boldsymbol{E}_\omega(\boldsymbol{F})\boldsymbol{A}_v(\omega)\boldsymbol{x}_v(t)\\ &= \boldsymbol{A}_0(\boldsymbol{F})\boldsymbol{E}_\omega(\boldsymbol{F})\boldsymbol{x}_v(t) + \boldsymbol{A}_\tau(\boldsymbol{F})\boldsymbol{E}_\omega(\boldsymbol{F})e^{-\boldsymbol{A}_v(\omega)\tau}\boldsymbol{x}_v(t)\\ &\quad + \boldsymbol{B}_0(\boldsymbol{F})\boldsymbol{C}_v\boldsymbol{x}_v(t) + \boldsymbol{B}_\tau(\boldsymbol{F})\boldsymbol{C}_v e^{-\boldsymbol{A}_v(\omega)\tau}\boldsymbol{x}_v(t)\end{aligned}$$

As this should hold for all t, and hence all $\boldsymbol{x}_v(t)$, (11) follows. □

The matrix $\boldsymbol{E}_\omega(\boldsymbol{F})$ completely defines the frequency response of (5). More precisely, (10) implies that the transfer function $T_i(s)$ from v to the ith state x_i has the magnitude and phase:

$$|T_i(j\omega)| = [E_{\omega,i1}(\boldsymbol{F})^2 + E_{\omega,i2}(\boldsymbol{F})^2]^{1/2} \tag{12}$$

$$\tan(\arg\ T_i(\omega)) = E_{\omega,i1}(\boldsymbol{F})/E_{\omega,i2}(\boldsymbol{F}) \tag{13}$$

where $E_{\omega,ij}(\cdot)$ denotes the ijth element of $\boldsymbol{E}_\omega(\cdot)$.

The controller design procedure studied in Section 3 is based on quadratic, frequency-dependent costs of the form:

$$J(\boldsymbol{F}, \omega) = \|T(j\omega)\|^2 \tag{14}$$

where $T(\cdot)$ denotes the transfer function from v to z,

$$\begin{aligned}T(s) &= \boldsymbol{C}(\boldsymbol{F})[s\boldsymbol{I} - \boldsymbol{A}_0(\boldsymbol{F}) - \boldsymbol{A}_\tau(\boldsymbol{F})e^{-s\tau}]^{-1}\\ &\quad \times [\boldsymbol{B}_0(\boldsymbol{F}) + \boldsymbol{B}_\tau(\boldsymbol{F})e^{-s\tau}] + \boldsymbol{D}(\boldsymbol{F})\end{aligned} \tag{15}$$

It follows from theorem 1 that the quadratic cost (14) can be expressed as:

$$\begin{aligned}J(\boldsymbol{F}, \omega) &= \mathrm{tr}[\boldsymbol{C}(\boldsymbol{F})\boldsymbol{E}_\omega(\boldsymbol{F}) + \boldsymbol{D}(\boldsymbol{F})\boldsymbol{C}_v]^T\\ &\quad \times [\boldsymbol{C}(\boldsymbol{F})\boldsymbol{E}_\omega(\boldsymbol{F}) + \boldsymbol{D}(\boldsymbol{F})\boldsymbol{C}_v]\end{aligned} \tag{16}$$

In the Appendix it is shown that the gradient of $J(\boldsymbol{F}, \omega)$ with respect to the controller parameter matrix $\boldsymbol{F}$ is given by:

$$\begin{aligned}\frac{\partial J(\boldsymbol{F}, \omega)}{\partial \boldsymbol{F}} &= 2\Big[\boldsymbol{D}_{12}^T[\boldsymbol{C}(\boldsymbol{F})\boldsymbol{E}_\omega(\boldsymbol{F}) + \boldsymbol{D}(\boldsymbol{F})\boldsymbol{C}_v] + \boldsymbol{B}_{21}^T\boldsymbol{L}_\omega(\boldsymbol{F})\\ &\quad + \boldsymbol{B}_{22}^T\boldsymbol{L}_\omega(\boldsymbol{F})e^{-\boldsymbol{A}_v(\omega)^T\tau}\Big][\boldsymbol{C}_2\boldsymbol{E}_\omega(\boldsymbol{F}) + \boldsymbol{D}_{21}\boldsymbol{C}_v]^T\end{aligned} \tag{17}$$

where the $\dim(\boldsymbol{x}) \times 2$ matrix $\boldsymbol{L}_\omega(\boldsymbol{F})$ is given by the linear matrix equation:

$$\begin{aligned}&\boldsymbol{A}_0(\boldsymbol{F})^T\boldsymbol{L}_\omega(\boldsymbol{F}) + \boldsymbol{A}_\tau(\boldsymbol{F})^T\boldsymbol{L}_\omega(\boldsymbol{F})e^{-\boldsymbol{A}_v(\omega)^T\tau} - \boldsymbol{L}_\omega(\boldsymbol{F})\boldsymbol{A}_v(\omega)^T\\ &\quad + \boldsymbol{C}(\boldsymbol{F})^T[\boldsymbol{C}(\boldsymbol{F})\boldsymbol{E}_\omega(\boldsymbol{F}) + \boldsymbol{D}(\boldsymbol{F})\boldsymbol{C}_v] = 0\end{aligned} \tag{18}$$

Notice that the expressions (16)–(18) are closely related to the linear matrix equations used to evaluate quadratic costs in linear quadratic control. Various optimisation-based controller design methods which have been applied to parametric linear quadratic control [14] can therefore be adapted in a straightforward way to problems involving frequency-domain criteria as well.

3 Iterative design by multiobjective optimisation

In practice the appropriate bounds in (1) for the frequency response functions are not known *a priori*. Instead, the design process is iterative in nature, and the solution is determined by finding a controller which gives satisfactory values for all performance criteria. In this Section an interactive procedure is given, by which the controller specifications can be achieved.

Consider the closed-loop system (cf. (5))

$$\begin{aligned}\dot{\boldsymbol{x}}(t) &= \boldsymbol{A}_0(\boldsymbol{F})\boldsymbol{x}(t) + \boldsymbol{A}_\tau(\boldsymbol{F})\boldsymbol{x}(t-\tau) + \boldsymbol{B}_{0,i}(\boldsymbol{F})v_i(t) \\ &\quad + \boldsymbol{B}_{\tau,i}(\boldsymbol{F})v_i(t-\tau) \\ z_i(t) &= \boldsymbol{C}_i(\boldsymbol{F})\boldsymbol{x}(t) + \boldsymbol{D}_i(\boldsymbol{F})v_i(t), \quad i = 1, \ldots, N\end{aligned} \tag{19}$$

Define the associated transfer functions $\boldsymbol{T}_i(s)$, $i = 1, \ldots, N$, relating the inputs v_i to the outputs z_i, and the frequency-dependent costs:

$$J_i(\boldsymbol{F}, \omega) = \|T_i(j\omega)\|^2, \quad i = 1, \ldots, N \tag{20}$$

The design objective is to find a controller which achieves satisfactory values for all the costs $J_i(\boldsymbol{F}, \omega)$. An iterative, interactive procedure for the iterative design of a satisfactory controller can be described as follows [12, 15]. At each stage k, a controller $\boldsymbol{F}^k$ is assumed given, and the costs $\{J_i(\boldsymbol{F}^k, \omega)\}$ are presented to the designer. If the design is not satisfactory, a new controller $\boldsymbol{F}^{k+1}$ is determined in such a way that a more satisfactory solution is obtained. This can be achieved by specifying frequency intervals where the various costs should be reduced. In the remaining frequency ranges, appropriate upper bounds on the costs are specified in order to avoid unacceptably large values. A constrained optimisation problem is then formulated and solved in such a way that the specified cost reductions are achieved subject to the frequency-domain constraints. The proposed algorithm can be summarised as follows.

Algorithm

Step 0: Specify the set of costs $J_i(\boldsymbol{F}, \omega)$, $i \in I = \{1, \ldots, N\}$ and determine a stabilising controller with the associated feedback matrix $\boldsymbol{F}^0$. Set $k = 0$ and go to step 1.

Step 1: Calculate the costs $J_i(\boldsymbol{F}^k, \omega)$, and ask the following question: is there a set $I^k \subset I$ of costs $J_i(\boldsymbol{F}, \omega)$, $i \in I^k$, and frequency ranges Ω_i^k such that $\{J_i(\boldsymbol{F}, \omega)\}$, $i \in I^k$, $\omega \in \Omega_i^k$, should be decreased at the expense of other costs? If not, stop; $\boldsymbol{F}^k$ is then a satisfactory solution of the control problem.

Else, specify the set I^k and define a set $I_c^k \subset I$ of costs $J_i(\boldsymbol{F}, \omega)$, $i \in I_c^k$, and frequency ranges $\Omega_{c,i}^k$ such that $\{J_i(\boldsymbol{F}, \omega)\}$, $i \in I_c^k$, $\omega \in \Omega_{c,i}^k$, are allowed to increase. Specify the allowed maximum relative increase $\delta_i^k(\omega)$, $i \in I_c^k$ of the costs and go to step 2.

Step 2: Define the functions

$$J_i(\boldsymbol{F}) = \max\{J_i(\boldsymbol{F}, \omega) \quad : \quad \omega \in \Omega_i^k\}, \quad i \in I^k \tag{21}$$

and solve the constrained optimisation problem:

$$\min_{\boldsymbol{F}} \quad \max\{J_i(\boldsymbol{F})/J_i(\boldsymbol{F}^k) \quad : \quad i \in I^k\} \tag{22}$$

subject to

$$J_i(\boldsymbol{F}, \omega) \le (1 + \delta_i^k(\omega))J_i(\boldsymbol{F}^k, \omega), \quad \omega \in \Omega_{c,i}^k, \ i \in I_c^k \tag{23}$$

Take $\boldsymbol{F}^{k+1}$ as the solution of the optimisation problem. Set $k \leftarrow k + 1$ and go to step 1.

End of algorithm

Remark 1: Notice that the minimax cost (22) is defined in such a way that the costs $J_i(\boldsymbol{F})$ in the set $i \in I^k$ which are to be reduced are weighted relative to their previous values. In this way the solution of the optimisation problem results in a simultaneous reduction of all the costs in the set I^k, if such a reduction is possible [12].

In order to solve the constrained minimax optimisation problem defined by (22) and (23) it is useful to state it in the equivalent form:

$$\min_{q, \boldsymbol{F}} \quad \frac{1}{2} q^2 \tag{24}$$

subject to

$$\begin{aligned} a_i^k J_i(\boldsymbol{F}, \omega) - q &\le 0, \quad \omega \in \Omega_i^k, \ i \in I^k \\ J_i(\boldsymbol{F}, \omega) - c_i^k(\omega) &\le 0, \quad \omega \in \Omega_{ci}^k, \ i \in I_c^k \end{aligned} \tag{25}$$

where $a_i^k = 1/J_i(\boldsymbol{F}^k)$ and $c_i^k(\omega) = (1 + \delta_i^k(\omega))J_i(\boldsymbol{F}^k, \omega)$. The constrained optimisation problem (24), (25) can be solved by standard optimisation techniques. The frequency sets Ω_i, $\Omega_{c,i}$ usually consist of frequency intervals, and the optimisation problem is therefore an infinitely constrained optimisation problem. Efficient optimisation techniques for such problems exists, cf. for example [7]. The routine `fseminf` in the Matlab optimisation toolbox [16] gives a software implementation of infinitely constrained optimisation. The problem can be simplified by approximating the sets Ω_i, $\Omega_{c,i}$ by discrete sets consisting of a finite number of frequencies. The problem then reduces to a standard nonlinear constrained optimisation problem, which can be solved using standard optimisation software.

4 Examples

In this Section numerical examples are presented in order to demonstrate the use of the iterative design procedure described in Section 3. We consider the closed-loop depicted in Fig. 1, where it is assumed that G and G_d are single-input single-output systems.

A crucial step in the controller design process is the selection of the individual costs $J_i(\boldsymbol{F}, \omega)$ in (20). The closed-loop responses are characterised by the sensitivity function $S = 1/(1 + GK)$, the complementary sensitivity function $T = 1 - S$, and the control sensitivity function $S_u = KS$. It is therefore natural to include these transfer functions in the loop-shaping design.

In order to design a controller using the approach described in Section 3, it is necessary to know how the frequency responses affect the closed-loop behaviour, and what corresponds to a good design. Here we will use a set of quantitative frequency domain criteria proposed by [8] and [17]. They propose a tuning approach based on criteria defined in a low-frequency, medium-frequency, and high-frequency range. The frequency ranges are defined in such a way that the medium-frequency interval is a region in the vicinity of the plant crossover frequency. In the

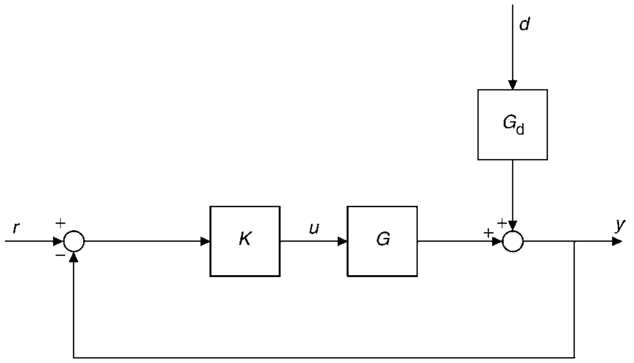

Fig. 1 *Closed-loop system*

low-frequency range $\omega \leq \omega_1$, the relevant performance measure is given by:

$$J_{\mathrm{LF}}(\boldsymbol{F}) = \max_{\omega}\left\{\left|\frac{G(j\omega)}{j\omega}S(j\omega)\right|^2 \quad : \quad \omega \leq \omega_1\right\} \qquad (26)$$

The cost $J_{\mathrm{LF}}(\boldsymbol{F})$ is a measure of the ability of the system to suppress low-frequency disturbances. A bounded value of the cost ensures that there are no steady-state offsets after step disturbances.

In the medium-frequency range $\omega \in [\omega_1, \omega_2]$, the important measures are given by

$$J_{\mathrm{MF},S}(\boldsymbol{F}) = \max_{\omega}\left\{|S(j\omega)|^2 \quad : \quad \omega \in [\omega_1, \omega_2]\right\} \qquad (27)$$

and

$$J_{\mathrm{MF},T}(\boldsymbol{F}) = \max_{\omega}\left\{|T(j\omega)|^2 \quad : \quad \omega \in [\omega_1, \omega_2]\right\} \qquad (28)$$

These measures are related to stability margins. The cost $J_{\mathrm{MF},S}(\boldsymbol{F})$ is equal to the square of the inverse of the shortest distance from $G(j\omega)K(j\omega)$ on the Nyquist curve to the critical point $(-1, 0)$. A reduction of the cost $J_{\mathrm{MF},T}(\boldsymbol{F})$ improves the phase margin and damping of the step response, without significantly slowing down the system response. For sufficient robustness, it has been recommended that $|S(j\omega)| \leq 1.7$ and $|T(j\omega)| \leq 1.3$ should hold.

Finally, robustness considerations motivate the high-frequency cost:

$$J_{\mathrm{HF}}(\boldsymbol{F}) = \max_{\omega}\left\{|K(j\omega)S(j\omega)|^2 \quad : \quad \omega \geq \omega_2\right\} \qquad (29)$$

A small value of $J_{\mathrm{HF}}(\boldsymbol{F})$ is required for good robustness to unmodelled high-frequency dynamics and in order to restrict control excitations due to high-frequency noise.

The frequency-domain objectives are coupled and the loops cannot therefore be shaped independently of one another. The problem of finding a controller which achieves satisfactory values for all the control performance measures can be solved by the iterative design procedure described in Section 3.

The following examples demonstrate how the proposed iterative design procedure can be applied. The first example considers a benchmark PID control problem for a non-minimum phase system. It is shown how the design can be improved in the desired direction by specifying the constrained optimisation problem in stage 2 of the algorithm. In the second example the proposed design procedure is applied to a complex industrial control problem consisting in the speed control of a diesel engine modelled as a poorly damped sixth-order system.

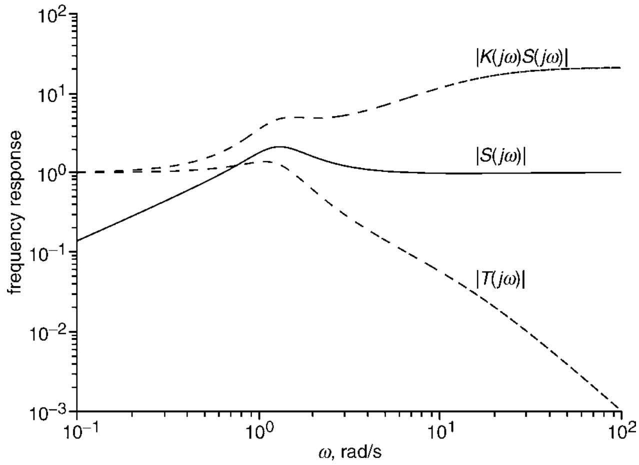

Fig. 2 *Frequency responses when using a PID controller with Ziegler-Nichols settings for the system (30)*

Example 1: Consider the control of the non-minimum phase system [8]

$$G(s) = \frac{1 - 0.5s}{(s+1)^3}, \qquad G_{\mathrm{d}}(s) = G(s) \qquad (30)$$

using a PID controller,

$$K(s) = K_{\mathrm{P}}\left(1 + \frac{1}{T_{\mathrm{I}}s} + \frac{T_{\mathrm{D}}s}{T_{\mathrm{f}}s + 1}\right) \qquad (31)$$

As an initial controller $\boldsymbol{F}^0$ we take a PID controller with Ziegler-Nichols controller settings, which are $K_{\mathrm{P}} = 1.92$, $T_{\mathrm{I}} = 2.65$, $T_{\mathrm{D}} = 0.66$. Using $T_{\mathrm{f}} = T_{\mathrm{D}}/10$, the closed-loop frequency responses are shown in Fig. 2, and the unit step responses are given in Fig. 3.

Suppose we wish to improve the pass-band robustness and the damping by reducing the medium-frequency criteria $J_{\mathrm{MF},S}(\boldsymbol{F})$ and $J_{\mathrm{MF},T}(\boldsymbol{F})$ at the expense of the low-frequency criterion $J_{\mathrm{LF}}(\boldsymbol{F})$, but without increasing the high-frequency cost $J_{\mathrm{HF}}(\boldsymbol{F})$. This can be achieved using the algorithm in Section 3. In this approach, an improved controller $\boldsymbol{F}$ is computed by solving the minimisation problem:

$$\min_{\boldsymbol{F}} \quad \max\left\{\frac{J_{\mathrm{MF},S}(\boldsymbol{F})}{J_{\mathrm{MF},S}(\boldsymbol{F}^0)}, \frac{J_{\mathrm{MF},T}(\boldsymbol{F})}{J_{\mathrm{MF},T}(\boldsymbol{F}^0)}\right\} \qquad (32)$$

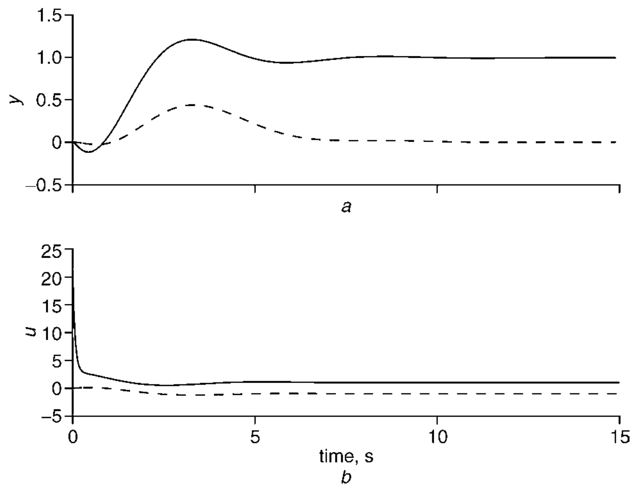

Fig. 3 *Step responses when using a PID controller with Ziegler-Nichols settings for the system (30)*

a y as a function of time
b u as a function of time

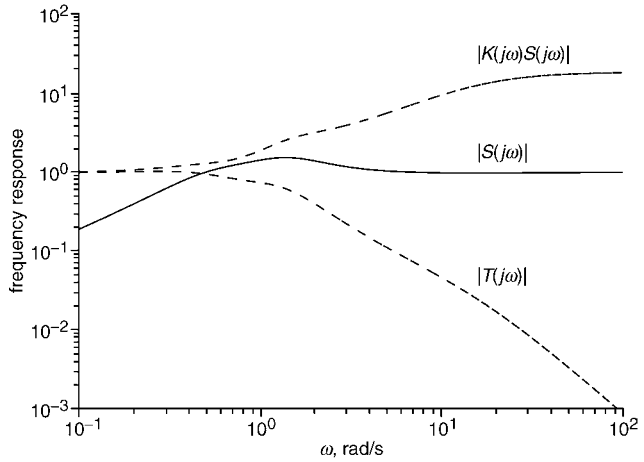

Fig. 4 *Frequency responses when using the improved PID controller for the system (30)*

subject to

$$J_{\mathrm{LF}}(\boldsymbol{F}) \leq (1+\delta_{\mathrm{LF}})J_{\mathrm{LF}}(\boldsymbol{F}^0)$$

$$J_{\mathrm{HF}}(\boldsymbol{F}) \leq (1+\delta_{\mathrm{HF}})J_{\mathrm{HF}}(\boldsymbol{F}^0)$$

The frequency ranges were defined by specifying the medium-frequency range as $[\omega_1, \omega_2] = [0.4, 3.0]$. In the optimisation problem, $\delta_{\mathrm{LF}} = 1$ and $\delta_{\mathrm{HF}} = 0$ were used. Hence, the low-frequency cost is allowed to increase by the factor two, whereas the high-frequency cost is not allowed to increase. The closed-loop responses achieved with the controller obtained by solving the above optimisation problem are shown in Figs. 4 and 5. It is seen that the shapes of the frequency responses are affected according to the specifications, resulting in reduced medium-frequency costs and better damping. The optimisation can be continued with further shaping of the closed-loop response until a satisfactory control performance is achieved.

Example 2: In this example, a more complex system is studied. The speed control system of a large marine diesel engine can be described by Fig. 1, where y is the angular velocity to be controlled, u is the position of the fuel rack

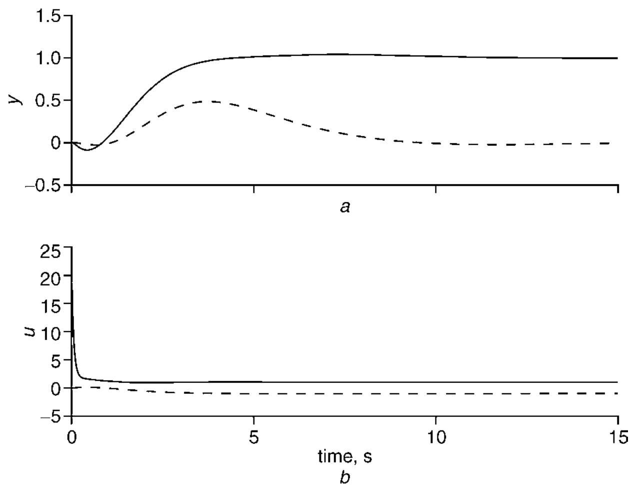

Fig. 5 *Step responses when using the improved PID controller for the system (30)*

a y as a function of time
b u as a function of time

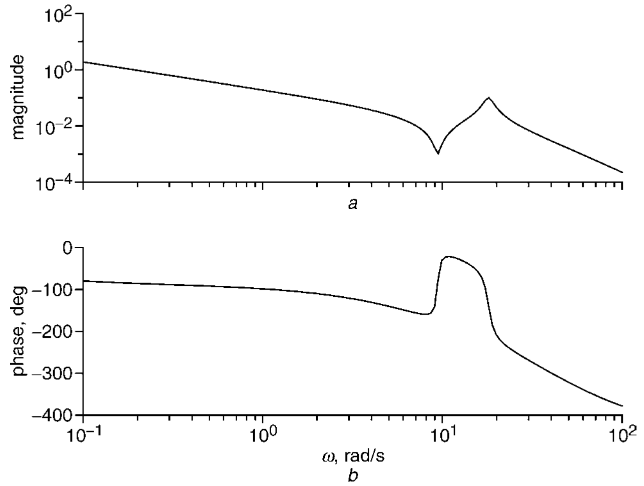

Fig. 6 *Bode plot of the transfer function (33)*

a Magnitude as a function of ω
b Phase as a function of ω

which is used as control signal, and d is the torque of the external load. The transfer functions are given by [18]:

$$G(s) = \frac{B_1(s)}{(\tau_1 s+1)(\tau_2 s+1)(\tau_3 s+1)A(s)} \quad (33)$$

$$G_{\mathrm{d}}(s) = \frac{B_2(s)}{A(s)} \quad (34)$$

where $\tau_1 = 0.0243$, $\tau_2 = 0.025$, $\tau_3 = 0.12$, and

$$B_1(s) = 0.693(s^2 + 0.520s + 87.72)$$

$$B_2(s) = -4(s + 170.7) \quad (35)$$

$$A(s) = (s + 0.0174)(s^2 + 1.927s + 322.6)$$

The control objective is to achieve a fast response to external disturbances, subject to constraints on the control action and a sufficient degree of robustness. Due to a flexible coupling between the engine and generator shafts the system is strongly oscillatory, having poles at $-0.9634 \pm 17.94j$. It is evident from the Bode plot of G shown in Fig. 6 that

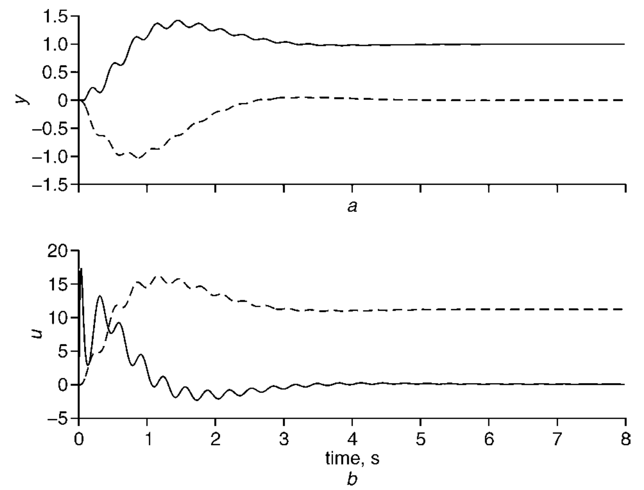

Fig. 7 *Step responses in example 2 when using a sixth-order controller tuned for load changes. The variables y and u represent deviations from nominal values*

a y as a function of time
b u as a function of time

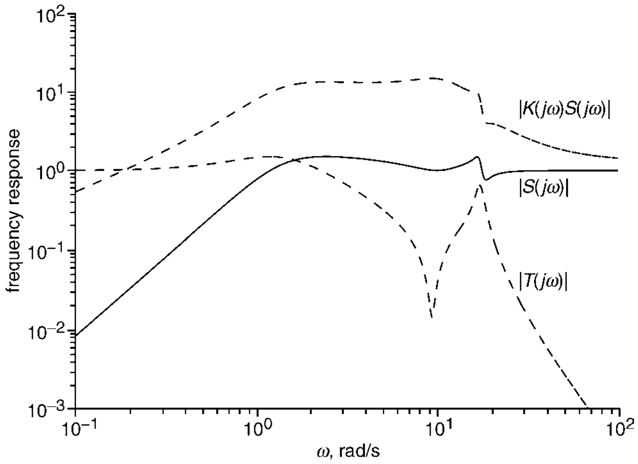

Fig. 8 *Frequency responses when using the optimised controller (36) in example 2*

the system is quite difficult to control. In particular, it is not possible to achieve satisfactory control performance with a PID controller. The actual engine installation was controlled using a sixth-order controller, which had been carefully tuned to give acceptable time responses for load changes in the disturbance d. However, frequency-domain criteria are not considered in the design, and due to poor damping the closed-loop response to setpoint changes is oscillatory, cf. Fig. 7. The poor damping and robustness properties are reflected by the frequency responses, which reveal that the controller achieves the medium-frequency performance levels $|S(j\omega)| \le 2.77$ and $|T(j\omega)| \le 2.04$, and a high-frequency cost with $|K(j\omega)S(j\omega)| = 12.8$ at $\omega = 100$ rad/s.

In order to improve the control performance the design procedure described in Section 3 was applied. The objective was to achieve improved stability margins without slowing down the time responses. Moreover, it was of interest to investigate whether the system could be controlled satisfactorily using a reduced-order controller. It was found that in order to achieve an acceptable performance, a controller of order three or higher is required. However, only marginal improvements can be obtained by using a controller order

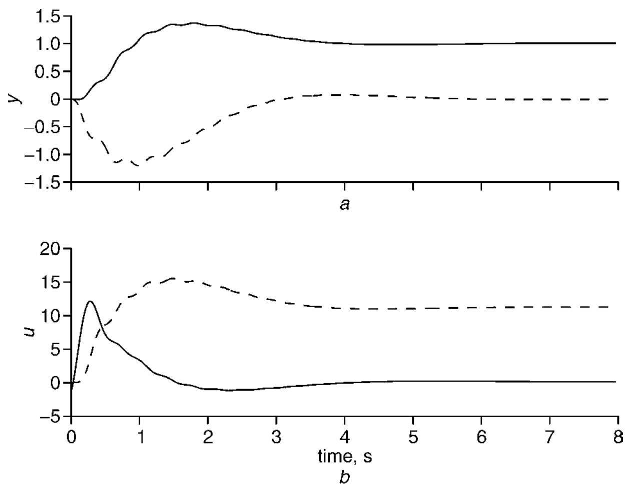

Fig. 9 *Step responses when using the optimised controller (36) in example 2. The variables y and u represent deviations from nominal values*

a y as a function of time
b u as a function of time

exceeding three. Figures 8 and 9 show the closed-loop responses of the optimised third-order controller:

$$K(s) = \frac{-1.31(s - 38.6)(s + 17.27)(s + 0.807)}{s(s^2 + 7.25s + 111)} \quad (36)$$

The controller was found after six iterations of the procedure, starting from an initial stabilising non-optimal controller. It is seen that improved stability margins and better damping have been achieved. The medium-frequency performance measures have been reduced to $|S(j\omega)| \le 1.50$ and $|T(j\omega)| \le 1.50$, and the high-frequency cost has the value $|K(j\omega)S(j\omega)| = 1.44$ at $\omega = 100$ rad/s.

The results show that with the iterative optimization-based controller design method it has been possible to reduce the controller order and obtain improved stability margins and robustness properties, while achieving time responses which are comparable to or better than the ones obtained with the original controller.

5 Conclusions

A multiobjective controller design procedure based on frequency-domain criteria has been proposed. The method is based on the solution of a sequence of constrained optimisation problems, which are defined in such a way that a more satisfactory design (in terms of the design specifications) is obtained in each iteration. Computational experience shows that in many cases a small number of iterations is sufficient to find a satisfactory design.

The proposed method is based on parametric optimisation techniques similar to those applied in parametric LQ control. The procedure thus allows the design of fixed-structure controllers, such as PID controllers. A key step of the procedure is the solution of a parametric optimisation problem with frequency-domain constraints. A particular feature of the approach is that the frequency responses are optimised directly, without the need to introduce any weighting filters. For this purpose, time-domain expressions for the frequency-domain costs and their gradients have been derived. This allows the use of powerful numerical gradient-based optimisation techniques.

If required, it is straightforward to generalise the procedure to more general frequency-domain performance measures (cf. [8]), or to include other types of costs, such as LQ costs.

6 Acknowledgment

Stefan Tötterman was supported by the Finnish Graduate School in Chemical Engineering (GSCE).

7 References

1 Bode, H.W.: 'Network Analysis and Feedback Amplifier Design' (D. Van Nostrand, 1945)
2 Horowitz, I.M.: 'Synthesis of Feedback Systems' (Academic Press, 1963)
3 McFarlane, D.C., and Glover, K.: 'Robust Controller Design Using Normalized Coprime Factor Plant Descriptions' (Springer-Verlag, 1990)
4 Skogestad, S., and Postlethwaite, I.: 'Multivariable Feedback Control' (Wiley, 1996)
5 Gahinet, P., and Apkarian, P.: 'A linear matrix inequality approach to $\mathcal{H}_\infty$-control', *Int. J. Robust Nonlinear Control*, 1994, **4**, pp. 421–448
6 Iwasaki, T.: 'A Unified Matrix Inequality Approach to Linear Control Design'. PhD Thesis, Purdue University, 1993
7 Polak, E., and Mayne, D.Q.: 'An algorithm for optimization problems with functional inequality constraints', *IEEE Trans. Autom. Control*, 1976, **21**, pp. 184–193

8 Lennartson, B., and Kristiansson, B.: 'Pass band and high frequency robustness for PID control'. Presented at the *36th IEEE Conf. on Decision and Control*, San Diego, CA, December 1997
9 Zadeh, L.A.: 'Optimality and non-scalar-valued performance criteria', *IEEE Trans. Autom. Control*, 1963, **8**, pp. 59–60
10 Salukvadze, M.E.: 'Vector-Valued Optimization in Control Theory' (Academic Press, 1979)
11 Kreisselmeier, G., and Steinhauser, R.: 'Application of vector performance optimization to a robust control loop design for a fighter aircraft', *Int. J. Control*, 1983, **37**, pp. 251–284
12 Toivonen, H.T., and Mäkilä, P.M.: 'Computer-aided design procedure for multi-objective LQG control problems', *Int. J. Control*, 1989, **49**, pp. 655–666
13 Khargonekar, P.P., and Rotea, M.A.: 'Multiple objective optimal control of linear systems: the quadratic norm case', *IEEE Trans. Autom. Control*, 1991, **36**, pp. 14–24
14 Mäkilä, P.M., and Toivonen, H.T.: 'Computational methods for parametric LQ problems–a survey', *IEEE Trans. Autom. Control*, 1987, **32**, pp. 658–671
15 Sawaragi, Y., Nakayama, H., and Tanino, T.: 'Theory of Multiobjective Optimization' (Academic Press, 1985)
16 Grace, A.: 'Optimization toolbox for use with MATLAB' (The MathWorks Inc., Natick, MA, 1994)
17 Kristiansson, B., and Lennartson, B.: 'Robust and optimal tuning for PI and PID controllers', *IEE Proc., Control Theory Appl.*, 2002, **149**, (1), pp. 17–25
18 Nuortio, A.: 'Modelling, Simulation and Control of Large Scale Diesel Engines'. MSc Thesis, Åbo Akademi University, 2000

8 Appendix

Proof of (17): From (16) we have:

$$\frac{\partial J(\boldsymbol{F},\omega)}{\partial \boldsymbol{F}} = 2\boldsymbol{D}_{12}^T[\boldsymbol{C}(\boldsymbol{F})\boldsymbol{E}_\omega(\boldsymbol{F}) + \boldsymbol{D}(\boldsymbol{F})\boldsymbol{C}_v] \times [\boldsymbol{C}_2\boldsymbol{E}_\omega(\boldsymbol{F}) + \boldsymbol{D}_{21}\boldsymbol{C}_v]^T + \boldsymbol{X} \qquad (37)$$

where the matrix $\boldsymbol{X} = [X_{ij}]$ is defined as:

$$\boldsymbol{X} = 2\left[\mathrm{tr}[\boldsymbol{C}(\boldsymbol{F})\boldsymbol{E}_\omega(\boldsymbol{F}) + \boldsymbol{D}(\boldsymbol{F})\boldsymbol{C}_v]^T \boldsymbol{C}(\boldsymbol{F})\frac{\partial \boldsymbol{E}_\omega(\boldsymbol{F})}{\partial F_{ij}}\right] \qquad (38)$$

By (18),

$$\boldsymbol{X} = 2\left[\mathrm{tr}\left(\boldsymbol{L}_\omega^T(\boldsymbol{F})\left(-\boldsymbol{A}_0(\boldsymbol{F})\frac{\partial \boldsymbol{E}_\omega(\boldsymbol{F})}{\partial F_{ij}} - \boldsymbol{A}_\tau(\boldsymbol{F})\frac{\partial \boldsymbol{E}_\omega(\boldsymbol{F})}{\partial F_{ij}}e^{-\boldsymbol{A}_v(\omega)\tau} + \frac{\partial \boldsymbol{E}_\omega(\boldsymbol{F})}{\partial F_{ij}}\boldsymbol{A}_v(\omega)\right)\right)\right] \qquad (39)$$

From (11) we have the identity

$$\begin{aligned} 0 &= \left[\mathrm{tr}\left(\boldsymbol{L}_\omega(\boldsymbol{F})^T \frac{\partial}{\partial F_{ij}}\left[\boldsymbol{A}_0(\boldsymbol{F})\boldsymbol{E}_\omega(\boldsymbol{F}) + \boldsymbol{A}_\tau(\boldsymbol{F})\boldsymbol{E}_\omega(\boldsymbol{F})e^{-\boldsymbol{A}_v(\omega)\tau} - \boldsymbol{E}_\omega(\boldsymbol{F})\boldsymbol{A}_v(\omega) + \boldsymbol{B}_0(\boldsymbol{F})\boldsymbol{C}_v + \boldsymbol{B}_\tau(\boldsymbol{F})\boldsymbol{C}_v e^{-\boldsymbol{A}_v(\omega)\tau}\right]\right)\right] \\ &= \left[\mathrm{tr}\left(\boldsymbol{L}_\omega(\boldsymbol{F})^T\left(\boldsymbol{A}_0(\boldsymbol{F})\frac{\partial \boldsymbol{E}_\omega(\boldsymbol{F})}{\partial F_{ij}} + \boldsymbol{A}_\tau(\boldsymbol{F})\frac{\partial \boldsymbol{E}_\omega(\boldsymbol{F})}{\partial F_{ij}}e^{-\boldsymbol{A}_v(\omega)\tau} - \frac{\partial \boldsymbol{E}_\omega(\boldsymbol{F})}{\partial F_{ij}}\boldsymbol{A}_v(\omega)\right)\right)\right] + [\boldsymbol{B}_{21}^T\boldsymbol{L}_\omega(\boldsymbol{F}) + \boldsymbol{B}_{22}^T\boldsymbol{L}_\omega(\boldsymbol{F})e^{-\boldsymbol{A}_v^T\tau}] \\ &\quad \times [\boldsymbol{C}_2\boldsymbol{E}_\omega(\boldsymbol{F}) + \boldsymbol{D}_{21}\boldsymbol{C}_v]^T \end{aligned}$$

Hence

$$\boldsymbol{X} = 2[\boldsymbol{B}_{21}^T\boldsymbol{L}_\omega(\boldsymbol{F}) + \boldsymbol{B}_{22}^T\boldsymbol{L}_\omega(\boldsymbol{F})e^{-\boldsymbol{A}_v^T\tau}][\boldsymbol{C}_2\boldsymbol{E}_\omega(\boldsymbol{F}) + \boldsymbol{D}_{21}\boldsymbol{C}_v]^T \qquad (40)$$

and (17) follows.